

Inhibition of calcium channel activation in GH3 cells by static magnetic fields

Arthur D. Rosen *

Department of Neurology, School of Medicine, State University of New York, Stony Brook, NY 11794-8121, USA

Received 14 November 1995; accepted 28 February 1996

Abstract

Voltage-activated calcium channel function was examined in cultured GH3 cells using the whole-cell patch clamp technique. Exposure to a 120 mT static magnetic field resulted in a slight reduction in the peak calcium current amplitude and shift in the current–voltage relationship. The most significant change was a slowing of the channel activation rate without any change in the inactivation rate. All changes in channel function were reversible, with return to pre-exposure values within 3 min after the field was turned off. These alterations in channel function were temperature-dependent. The present findings are consistent with a functional disruption of the intramembranous portion of the calcium channel by a magnetically induced membrane deformation.

Keywords: Static magnetic field; Calcium channel; GH3 cell

1. Introduction

Moderate intensity static magnetic fields (SMF) have been shown to influence a variety of biological systems. These include changes in the permeability of phospholipid bilayer membranes [1] inhibition of spontaneous neuronal activity in the central nervous system [2], disorganization of protozoan locomotion [3], alteration in the function of membrane-bound receptors in hemopoietic stem cells [4], inhibition of neurotransmitter release at the neuromuscular junction [5], and inhibition of neuronal action potentials in dissociated cultures of dorsal root ganglia neurons [6]. Most of the biological phenomena attributed to SMFs may be explained by changes in cellular calcium. It has been suggested [2] that SMFs induce a partial realignment of diamagnetically anisotropic molecules within the cell membrane, thereby distorting imbedded calcium channels sufficiently to alter their function. Support for this hypothesis has come from experimental studies which indirectly measured membrane calcium function [7]. An alternative hypothesis [8] proposes that the realignment of the membranes diamagnetically anisotropic molecules effects a release of membrane-bound calcium ions which then potenti-

ate Ca^{2+} -activated potassium channels, resulting in membrane hyperpolarization.

In order to achieve an understanding of those events occurring at the membrane in response to SMFs, it is necessary to directly measure specific membrane ionic currents. Such measurements are possible using the whole-cell patch clamp methodology. The present study employed this technique, with cultured GH3 cells, to examine calcium channel function in the presence of SMFs. The GH3 cell line is of pituitary origin and exhibits robust voltage-activated calcium currents [9]. It was in this cell line that low and high threshold calcium currents were originally described [10]. These cells also exhibit large tetrodotoxin (TTX)-sensitive sodium currents, characteristic of a neuronal phenotype [9], but do not elaborate neurites in culture. This obviates any potential complication involving spatial clamp of rapidly activated inward sodium or calcium current. In addition to studies of voltage-activated inward current, GH3 cells have proven useful for the study of calcium-activated potassium channel function and modulation [11,12]. Since GH3 cells are maintained in culture, they are especially amenable to whole-cell patch clamp methodology. This cell line, therefore, represents an ideal diagnostic tool for analysis of the effects of SMFs on voltage-dependent calcium channel function.

* Corresponding author. Fax: +1 (516) 4441474; e-mail: arosen@neuro.som.sunysb.edu.

2. Materials and methods

2.1. Cell cultures

Proliferating GH3 cells were grown in 100 mm polystyrene culture dishes at 37°C in a 5% CO₂ environment. The growth medium contained DMEM supplemented with 10% fetal calf serum and penicillin/streptomycin. As the cells approached confluency, they were split and replated at 10% of their initial density. At the same time a number of 35 mm polystyrene culture dishes were established to provide sufficient dishes of cells for recording on any given day. All recordings were carried out between two and five days of plating to minimize any variability due to cell health.

2.2. Exposure system

The electromagnet used in this study consisted of a 2700 turn coil wound on a 2.4 cm² soft iron C-core with an air gap of 44 mm. The coil was powered by a computer-controlled current source and the system could generate static fields with flux densities up to 125 mT. In order to eliminate any unwanted transients, the coil current was ramped on and off at 2.35 A/s. The magnet was mounted on a specially constructed aluminum stage designed to fit the Zeiss Axiovert 100 microscope. All ferromagnetic materials were removed or replaced on this microscope. Tissue culture dishes, placed on the thermoregulated portion of the microscope stage (stable to $\pm 0.1^\circ\text{C}$), were oriented horizontally between the poles of the magnet. Recordings were carried out on those cells within the 650 μm diameter microscope field, which was fixed in position and centered midway between the magnet poles. Precise measurements of the field generated by this

device have been carried out and a spatial plot, in the plane of the floor of the culture dish, is shown in Fig. 1. In the area of recording ($0 \pm 325 \mu\text{m}$), field nonhomogeneity was 0.2%. The microscope illuminator was operated from a well-filtered DC source and no stray fields could be detected from it or from the thermoregulation device. Heat generated by the magnet coils was dissipated well away from the cells from which recordings were made.

2.3. Recording conditions

Immediately prior to recording, the growth medium in a 35-mm culture dish was slowly exchanged with a recording solution consisting of 120 mM NaCl, 10 mM CaCl₂, 2 mM MgCl₂, 1 μM TTX, and 10 mM HEPES, titrated with NaOH to a pH of 7.2. The dish was then placed on the thermoregulated portion of the microscope stage.

Patch pipettes were pulled from borosilicate glass to an outer diameter of approx. 2 μm and lightly firepolished. The electrode was filled with a solution consisting of 120 mM CsCl, 10 mM K-EGTA, and 10 mM HEPES, titrated with KOH to a pH of 7.2. These electrodes were of low resistance (2–4 M Ω) which, along with the use of series resistance compensation, minimized voltage clamp errors due to excessive access resistance [13]. Membrane current was recorded with an Axopatch 1-D patch clamp amplifier. Command voltages for this amplifier were generated with HEKA Pulse software running on a Macintosh 840AV computer. Current responses were digitized at 40 kHz on an Instrutech ITC-16 A/D converter and processed for display by the Pulse software.

Under slight positive pressure, the electrode tip was lowered to the cell surface while its resistance was continuously monitored by measuring the current in response to application of a 10 mV, 10 ms pulse. Once the electrode

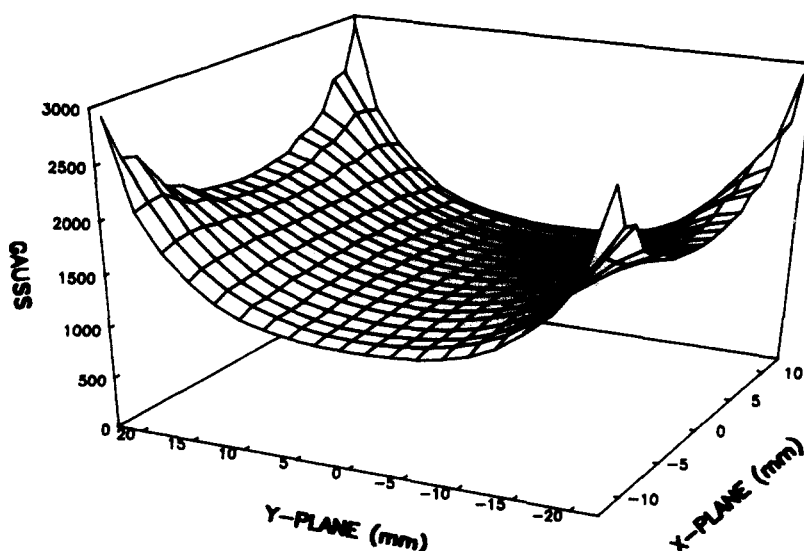


Fig. 1. Magnetic field measured normal to the inter-pole axis (Y-plane) at the level of the floor of the tissue culture dish. Measurements for mid-pole field of 1230 G (123 mT).

touched the cell a small negative pressure was applied in order to form a seal of at least $1\text{ G}\Omega$. Following seal formation, the tissue within the pipette was broken with additional suction or by voltage zap (1 V for 5 ms). The membrane was clamped to a holding potential of -80 mV , unless otherwise indicated, and inward calcium current was immediately assessed by application of a series of 100 ms test pulses in 5 mV increments from the holding potential to $+40\text{ mV}$. Correction for any linear leakage currents, was accomplished with a P/4 subtraction protocol [14]. This leak subtracted data was displayed along with on-line analysis of the current–voltage relations for that cell. Since a brief, but finite, period of time was necessary for the electrode solution to dialyze the intracellular solution, further analysis was delayed until the current–voltage relationship stabilized.

Once the system was stable, a 120 mT SMF was applied for 150 s. The voltage jump sequence was repeated beginning 100 s after the field was turned on and at 30 s, 100 s, and 170 s, after it was turned off. In most cells recordings were also obtained with the holding potential at -40 mV , in order to inactivate the low threshold T-type channels and allow evaluation of only L-type channels. The influence of temperature on SMF effect was examined by carrying out all studies at 23°C , 27°C , 32°C , and 37°C . Because of the amount of time necessary to acquire data

for each exposure sequence, as well as the time needed to change the bath temperature without damaging the cells ($0.5^\circ\text{C}/\text{min}$), it was not usually possible to record from the same cell at more than one temperature. In all cases both the data and current–voltage relations were displayed on-line and data stored for off-line analysis. Current–voltage plots could be regenerated from the stored data. In addition, activation and inactivation rates were computed off-line by fitting the calcium current at each voltage step with a general Hodgkin-Huxley formalism with a defined number of activation gates (three) and inactivation gates (one). The time constants τ_m and τ_h , thus generated define the activation and inactivation kinetics respectively.

3. Results

The present study was limited to examining the effects of SMFs on membrane calcium current in GH3 cells. Currents were measured in 37 cells using the whole-cell configuration of the patch clamp technique. Cells were of fairly uniform size, with an average diameter $15\text{ }\mu\text{m}$ and stable recordings were usually possible for periods of 10 to 15 min. Measurement of only inward calcium current was made possible by blocking both inward sodium current with external TTX, and outward potassium current with internal cesium and EGTA.

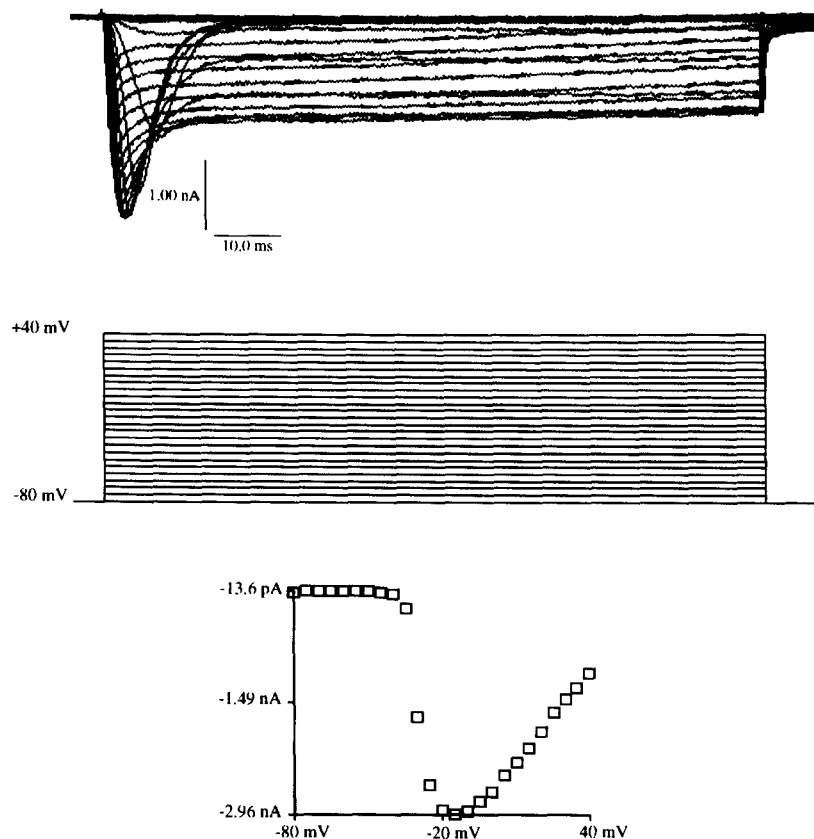


Fig. 2. Inward voltage-activated calcium current (top) in a GH3 cell at 27°C . 25 superimposed responses to a 100 ms voltage step sequence (middle) from a holding potential of -80 mV . Current–voltage relationship curve (bottom) reveals maximum inward current of 2.96 nA occurs at -15 mV .

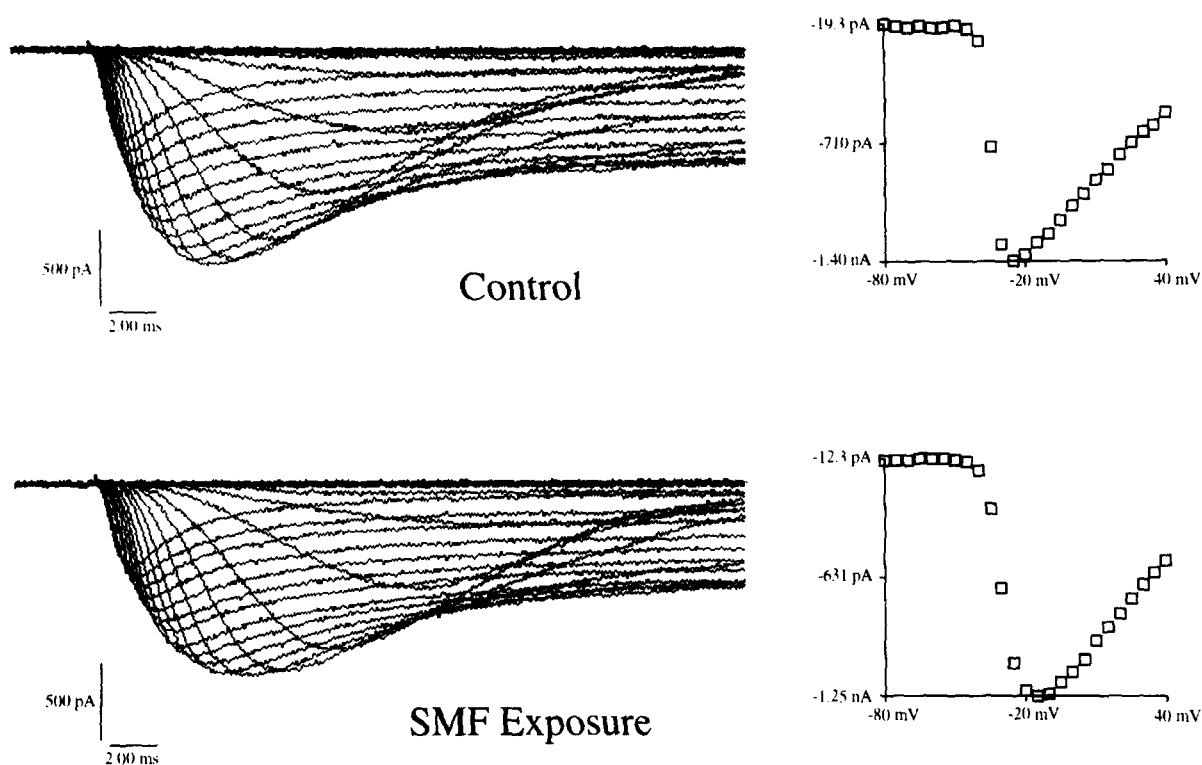


Fig. 3. Inward voltage-activated calcium current in GH3 cell at 27°C. Holding potential -80 mV. Small reduction in peak current amplitude and 10 mV shift in current-voltage relationship during 120 mT SMF exposure. Activation rate reduced during exposure. Exposure sequence began 100 s after field was turned on.

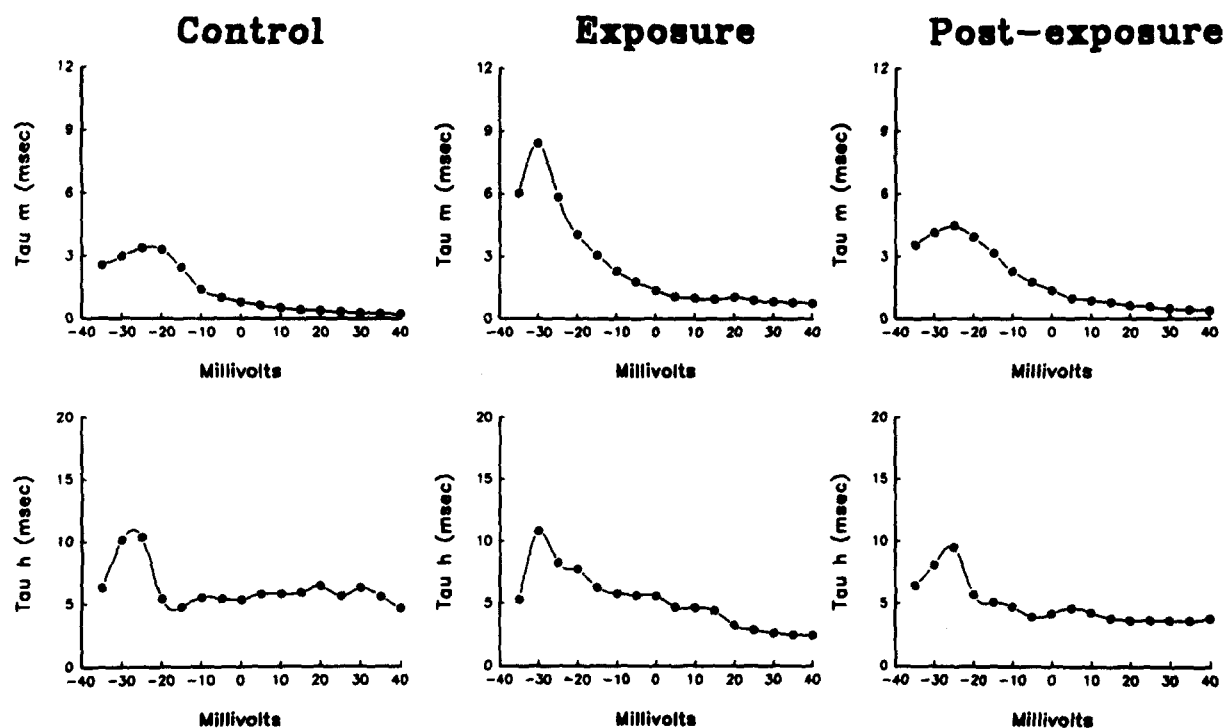


Fig. 4. Channel activation time constant (top) and inactivation time constant (bottom) for L-type calcium channels at 27°C before, during, and after exposure to a 120 mT SMF. Same cell as in Fig. 3 but with holding potential raised to -40 mV to inactivate T-type channels. Prominent slowing of activation during exposure with nearly complete return to control values 165 s following exposure. No significant change in inactivation.

The typical response to a 100-ms voltage step sequence is shown in Fig. 2. The initial rapidly activated inward calcium current peaked at approx. 5 ms and, almost as rapidly, decayed to 40–50% of the initial maximum value. The relationship between the peak current and the step voltage is also presented in Fig. 2 and reveals that, for this cell, the peak inward current occurred at -15 mV. This value varied somewhat from cell to cell but, for any given cell, remained constant with repeated testing.

During exposure to a 120 mT SMF, a shift in the current–voltage relationship was usually seen along with a small change in peak current amplitude. This is illustrated in Fig. 3. In that experiment, carried out at 27°C , the membrane holding potential was set at -80 mV, thereby allowing activation of both T- and L-type calcium channels. There was a 10-mV shift in the current–voltage relationship as well as a 143 pA reduction in peak current amplitude. Most impressive, however, was the slowing of the activation rate, evident on examination of the calcium current tracings. In order to quantify this change, activation and inactivation time constants were computed before, during and after exposure to the 120 mT SMF. These are shown in Fig. 4. This data is from the same cell shown in Fig. 3, but the membrane holding potential was raised to -40 mV in order to inactivate the low threshold T-type channels. An increase in the calcium channel activation time constant (τ_m) without significant change in the inactivation time constant (τ_h) is clearly seen. The change in τ_m was present at all levels of membrane depolarization, but was greatest between -35 mV and -15 mV, where it more than doubled. This was the most consistent change during SMF exposure and, as seen in Fig. 4, was fully reversible 2–3 min after the field was turned off. The increase in τ_m was found to be temperature-dependent. This is illustrated in Fig. 5, where mean values for both τ_m and τ_h , following membrane depolarization to -30 mV, were calculated during SMF exposure and compared to mean baseline values at the same temperature. The 12% increase in τ_m at 22°C was not statistically significant ($P = 0.65$) but the 124% increase at 27°C and the 130% increase at 32°C were ($P < 0.001$). The 91% increase in τ_m at 37°C was less impressive but still significant ($P = 0.05$). Changes in τ_h during SMF exposure were small and, in all cases, not statistically significant.

4. Discussion

The macroscopic current recorded from GH3 cells, using the whole-cell patch clamp methodology, represents the temporal integration of individual channel currents [15] and the behavior of this current may be modeled with the kinetics originally developed to explain action potential generation [16]. The voltage-activated currents recorded in this study are consistent with those described in the literature [9–11,17]. The use of appropriate recording and elec-

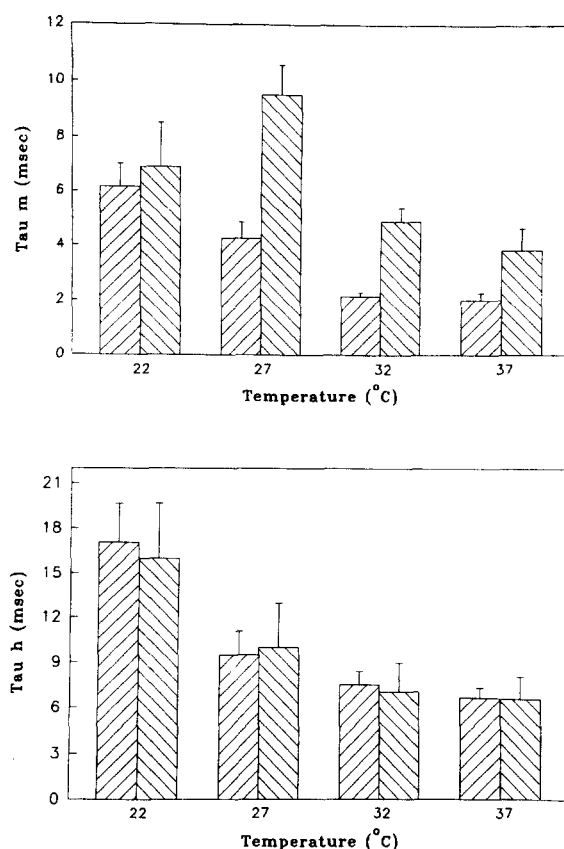


Fig. 5. Mean and standard error values for activation (top) and inactivation (bottom) time constants. L-type calcium channels activated at -30 mV, at temperatures of 22° , 27° , 32° , and 37°C . For each temperature, left bar represents values in the absence of SMF, right bar represents values during exposure to 120 mT field. Significant change in activation time constant during exposure only at 27° , 32° , and 37°C . No change in inactivation time constant at any temperature.

trode solutions assured that the only current present was that attributable to calcium. Inward sodium current was abolished by TTX, while outward potassium current was eliminated by replacing intracellular K^+ with Cs^+ , which has minimal mobility within potassium channels. In addition, Ca^{2+} -activated potassium channels were inhibited by intracellular EGTA which rapidly and selectively chelates Ca^{2+} . It has been shown that inward current remaining after the elimination of sodium current is abolished by the application of a number of different impermeant calcium channel blockers to the surface of the cell [11]. A consistent feature of our recordings was the early partial inactivation of inward calcium current. This has previously been described in GH3 cells [9] and since it is significantly reduced when Ba^{2+} is substituted for Ca^{2+} as the charge carrier, is regarded as Ca^{2+} -dependent inactivation.

Diamagnetic anisotropic molecules will experience translational movements in the presence of a strong magnetic field gradient. In a homogeneous field, however, they merely align to an orientation representing the minimum free energy state. This effect is small for individual

molecules and the randomizing effect of thermal energy is more than sufficient to prevent such reorientation. It has been shown [18] that for domains of interacting molecules, aligned along a common axis, individual anisotropies summate and may be sufficient to overcome the effects of thermal energy. Biological membranes, with their highly ordered phospholipid bilayer structure, exhibit substantial diamagnetic properties. The ratio of magnetic interaction energy to thermal energy is a measure of average molecular orientation may be expressed by the ratio, β , of magnetic to thermal energy.

$$\beta = \frac{-N\Delta_{\chi}H^2}{k_{\text{B}}T}$$

where N is the number of interacting molecules, each with a diamagnetic anisotropy Δ_{χ} , H is flux density, k_{B} is Boltzmann's constant and T is absolute temperature.

The actual molecular reorientation within a phospholipid bilayer is the balance between the theoretical value of β and those intermolecular forces which limit movement. At low temperatures the membrane exists in a gel phase with tight alignment of individual molecules, maintained by both intermolecular forces and the excluded volume effect of packed lipid molecules. With increasing temperature, an abrupt rotameric disordering of the lipid acyl chains occurs, marking the transition to the liquid-crystal phase. This less rigid membrane will be more readily deformed in a magnetic field and such deformity could alter the function of imbedded calcium channels.

Much of what we know about the relationship between structure and function in the calcium channel complex has been derived from work carried out on muscle. Although there are some tissue and species differences, a sufficient degree of homology exists to allow extrapolation to several other systems, including the GH3 cells used in the present study. Entry of calcium is essential for a variety of cellular functions including enzyme activation, membrane conductance, exocytosis, and motility. As a critical messenger for intracellular function, calcium entry into the cell is tightly regulated. The present study provides direct evidence that SMFs interfere with this regulation by inhibiting the calcium channel activation mechanism. Inhibition was present at all levels of membrane depolarization though, not surprisingly, was especially evident during partial depolarization when the intrinsic calcium kinetics are slow, and appears to take the form of a reduced probability of channel opening. In addition, the shift in the current–voltage relationship curve suggests that there is also a diminished channel voltage sensitivity. Activation of voltage-sensitive channels has been shown to be a function of the intramembranous portion of the channel. More specifically, it is the α_1 subunit that is the primary voltage-sensitive molecule in the calcium channel complex [19–21]. This is the largest (212 kDa) of the five proteins which make up the channel and is located almost entirely within

the membrane. As such, it would be expected to be especially vulnerable to any membrane deformation induced by an SMF.

This study did not demonstrate any change in the calcium channel inactivation rate. Two mechanisms for this inactivation have been described, one is voltage-dependent and the other is Ca^{2+} -dependent. Voltage-dependent inactivation has been linked to a peptide moiety in the membrane's cytoplasmic domain. Intracellular trypsin abolishes this form of inactivation as well as increasing the number of functional channels, thereby increasing inward calcium current several-fold [22]. This is similar to the 'ball and chain' model originally proposed for sodium channels [23]. Membrane deformation would have little, if any, effect on this mechanism. Ca^{2+} -dependent inactivation is a more rapid process, shown to be due to the inactivation of the calcium channel by entering Ca^{2+} [24]. The precise locus on the calcium channel complex where inactivation occurs has not been established. In order for there to be relative immunity to membrane deformation, however, it would have to be at either the intracellular or extracellular channel pore. The intracellular pore is formed by the β -subunit (57 kDa), while the extracellular pore consists of the α_2/δ -subunit (125 kDa), a disulfide-linked dimer. By genetically expressing various combinations of α_1 -, α_2/δ -, and β -subunits, it has been shown [25] that the co-expression of either the α_2/δ - or β -subunit along with the α_1 -subunit accelerated channel inactivation kinetics. Presumably, therefore, the site for Ca^{2+} -dependent inactivation is on either the α_2/δ -subunit or the β -subunit, or on both.

The present findings are consistent with the hypothesis that realignment of the membrane's diamagnetically anisotropic molecules impairs the activation of imbedded voltage-sensitive calcium channels while leaving unaffected those portions of the channel which do not lie within the membrane per se. The observed temperature dependence is presumably related to the membrane thermotropic phase transition, with the more fluid liquid-crystal membrane being more easily deformed in the presence of a strong SMF. This mechanism, which now has direct experimental support, is sufficient to explain the reported bioeffects of these fields. It is possible that additional mechanisms, including functional changes in potassium and/or sodium channels, may also be operative. Using the versatile technique of whole-cell patch clamp recording, such putative mechanisms can be evaluated, both in terms of existence and relative contribution to SMF effect.

Acknowledgements

This study was carried out during the tenure of NIH NRSA fellowship 1F33NS09544-01 and was made possible by the generous help of Dr. Paul Brehm whose labora-

tory, in the Department of Neurobiology and Behavior at the State University of New York at Stony Brook, is supported by NIH Grant NS18205.

References

- [1] Tenforde, T.S. and Liburdy, R.P. (1988) *J. Theor. Biol.* 133, 385–396.
- [2] Rosen, A.D. and Lubowsky, J. (1990) *Exp. Neurol.* 108, 261–265.
- [3] Rosen, M.S. and Rosen, A.D. (1990) *Life Sci.* 40, 1509–1515.
- [4] Peterson, H.-P., von Wangenheim, K.-H. and Feinendegen, L.E. (1992) *Radiat. Environ. Biophys.* 31, 31–38.
- [5] Rosen, A.D. (1992) *Am. J. Physiol.* 262 (Cell Physiol. 31), C1418–C1422.
- [6] McLean, M.J., Holcomb, R.R., Wamil, A.W., Pickett, J.D. and Cavopoli, A.V. (1995) *Bioelectromagnetics* 16, 20–32.
- [7] Rosen, A.D. (1994) *Biochim. Biophys. Acta* 1193, 62–66.
- [8] Azanza, M.J. and del Moral, A. (1994) *Progr. Neurobiol.* 44, 517–601.
- [9] Matteson, D.R. and Armstrong, C.M. (1984) *J. Gen. Physiol.* 83, 371–394.
- [10] Matteson, D.R. and Armstrong, C.M. (1986) *J. Gen. Physiol.* 87, 161–182.
- [11] Dubinsky, J.M. and Oxford, G.S. (1984) *J. Gen. Physiol.* 83, 309–339.
- [12] Ritchie, A. (1987) *J. Physiol.* 385, 591–609.
- [13] Sakmann, B. and Neher, E. (1985) *Single-Channel Recording*, pp. 28–29, Plenum Press, New York.
- [14] Bezanilla, F. and Armstrong, C.M. (1977) *J. Gen. Physiol.* 70, 549–566.
- [15] Fernandez, J.M., Fox, A.P. and Krasne, S. (1984) *J. Physiol.* 356, 565–585.
- [16] Hodgkin, A.L. and Huxley, A.F. (1952) *J. Physiol.* 117, 500–544.
- [17] Hagiwara, S. and Ohmori, H. (1982) *J. Physiol.* 331, 231–252.
- [18] Maret, G. and Dransfeld, K. (1977) *Physica* 86–88B, 1077–1083.
- [19] Mikami, A., Imoto, K., Tanabe, T., Niidome, T., Mori, Y., Takeshima, H., Narumiya, S. and Numa, S. (1989) *Nature* 340, 230–233.
- [20] Perez-Reyes, E., Wei, X., Castellano, A. and Birnbaumer, L. (1990) *J. Biol. Chem.* 265, 20430–20436.
- [21] Soong, T.W., Stea, A., Hodson, C.D., Dubel, S.J., Vincent, S.R. and Snutch, T.P. (1993) *Science* 260, 1133–1136.
- [22] Obejero-Paz, C.A., Jones, S.W. and Scarpa, A. (1991) *J. Gen. Physiol.* 98, 1127–1140.
- [23] Armstrong, C.M. and Bezanilla, F. (1977) *J. Gen. Physiol.* 70, 567–590.
- [24] Yue, D.T., Backx, P.H. and Imredy, J.P. (1990) *Science* 250, 1735–1738.
- [25] Welling, A., Bosse, E., Cavalie, A., Bottlender, R., Ludwig, A., Nastainczyk, W., Flockerzi, V. and Hofmann, F. (1993) *J. Physiol.* 471, 749–765.